J Physiol Sci (2010) 60:441–446
DOI 10.1007/s12576-010-0111-1

SHORT COMMUNICATION

Control of ionic selectivity by a pore helix residue in the Kv1.2 channel

Chia-Chia Chao · Chieh-Chen Huang · Chang-Shin Kuo · Yuk-Man Leung

Received: 27 June 2010 / Accepted: 24 August 2010 / Published online: 15 September 2010

Abstract Interaction between the selectivity filter and the adjacent pore helix of voltage-gated K^+ (Kv) channels controls pore stability during K^+ conduction. Kv channels, having their selectivity filter destabilized during depolarization, are said to undergo C-type inactivation. We examined the functionality of a residue at the pore helix of the Kv1.2 channel (V370), which reportedly affects C-type inactivation. A mutation into glycine (V370G) caused a shift in reversal potential from around −72 to −9 mV. The permeability ratios (P_{Na}/P_K) of the wild type and V370G mutant are 0.04 and 0.76, respectively. In the wild-type, P_{Rb}/P_K, P_{Cs}/P_K and P_{Li}/P_K are 0.78, 0.10 and 0.05, respectively. Kv1.2 V370G channels had enhanced permeability to Rb^+ and Cs^+ (P_{Rb}/P_K and P_{Cs}/P_K are 1.63 and 1.18, respectively); however, Li^+ permeability was not significantly augmented (P_{Li}/P_K is 0.13). Therefore, in addition to its known effect on pore stability, V370 of Kv1.2 is also crucial in controlling ion selectivity.

Keywords Voltage-gated K^+ channels · C-type inactivation · Selectivity filter · Permeability

C.-C. Chao · C.-C. Huang
Department of Life Sciences, National Chung Hsing University, Taichung 402, Taiwan

C.-C. Chao · C.-S. Kuo · Y.-M. Leung (✉)
Graduate Institute of Neural and Cognitive Sciences, China Medical University, Taichung 40402, Taiwan
e-mail: ymleung@mail.cmu.edu.tw

Introduction

Voltage-gated K^+ (Kv) channels are important in repolarization of neurons [1]. The ability of the Kv channel to permit massive yet selective K^+ flux relies on its selectivity filter, which has the T(V/I)GYG signature motif [2–4]. The selectivity filter of Kv channels is not an entirely rigid structure; it constricts or destabilizes during depolarization, a process termed C-type inactivation [5, 6]. The stability or conformation of the selectivity filter has a profound effect on ionic permeability. Thus, during C-type inactivation, the selectivity filter temporarily loses its K^+ selectivity as it constricts and allows Na^+ ions to pass through [7]. The interaction between the selectivity filter and the adjacent pore helix has been shown to be critical in controlling the stability of the selectivity filter during K^+ conduction. In the Kv1.2 channel, mutating Val370 into Glu370 strengthens the interaction with Asp379 to act as a molecular spring, distorting the selectivity filter and accelerating C-type inactivation [8]. A more dramatic change in flexibility of the selectivity filter of Kv channels has been demonstrated in a recent work by Fedida and colleagues [9]. In this report, Kv3.1 channels could be shown to conduct $NMDG^+$ in the absence of K^+. Such flexibility is attributable to a residue (Tyr407) at the outer pore. Kv1.5 did not display such a flexibility; however, a mutation at the homologous position of Kv1.5 (R487Y) endows the channel with $NMDG^+$ conductivity.

In this report, we examined the functionality of the residue located at the pore helix of Kv1.2, V370 (Fig. 1), which has previously been known to affect C-type inactivation [8, 10]. A mutation into glycine (V370G) allowed conduction of Na^+ as well as K^+, and this mutation also enhanced permeability to Rb^+ and Cs^+, but not Li^+.

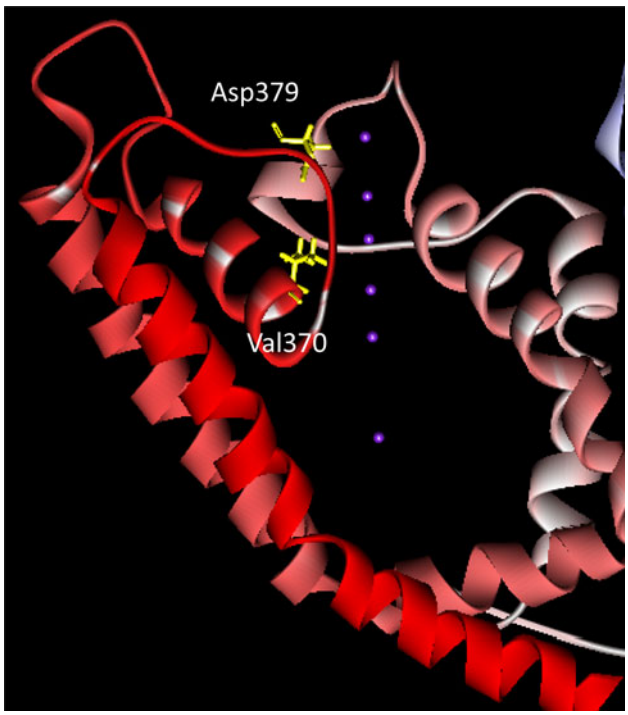

Fig. 1 Molecular graphics showing the pore helix and selectivity filter of the Kv1.2 channel. Val370 and Asp379 are indicated as *yellow sticks*

Our novel observations suggest that V370 of the Kv1.2 channel is important for ionic discrimination.

Materials and methods

Cell culture

Oral carcinoma OECM-1 cells were cultured at 37°C in 5% CO_2 in Roswell Park Memorial Institute 1640 medium (Invitrogen, Carlsbad, CA, USA) supplemented with 10% fetal bovine serum and penicillin–streptomycin (100 units/mL, 100 μg/mL) (Invitrogen).

Mutagenesis and transfection

pcDNA3.1-Kv1.2 was obtained from Prof. H. Gaisano (University of Toronto) and pEGFP (as marker) was purchased from Clontech, Palo Alto, CA, USA. Primers used were: forward (5′–3′) CTC CTT TGA GTT TCT GGT; reverse (5′–3′): ACT CTT ACC AAC CGG ATG. Mutation of pcDNA3.1-Kv1.2 wild-type (WT) into V370G and V370E was performed according to the protocols of QuikChange® II Site-Directed Mutagenesis Kit (Stratagene, La Jolla, CA, USA). The mutation was confirmed by DNA sequencing. For heterologous expression of Kv1.2 WT and mutant channels, the plasmids were transiently transfected into OECM-1 cells using TurboFect (Invitrogen) according to the manufacturer's instructions.

Electrophysiology

Electrophysiological experiments were performed as previously reported [10]. OECM-1 cells were voltage-clamped in the whole-cell configuration. Thin-walled borosilicate glass tubes (o.d. 1.5 mm, i.d. 1.10 mm; Sutter Instrument, Novato, CA, USA) were pulled with a micropipette puller (P-87; Sutter Instrument), and then heat polished by a microforge (Narishige Instruments, Sarasota, FL, USA). The pipettes, filled with intracellular solution, containing (mM): 140 KCl, 1 $MgCl_2$, 1 EGTA, 10 HEPES, and 5 MgATP (pH 7.25 adjusted with KOH), had typical resistance of 4-7 MΩ. The bath solution contained (mM): 140 NaCl, 4 KCl, 1 $MgCl_2$, 2 $CaCl_2$, 10 HEPES (pH 7.4 adjusted with NaOH). When permeability for other ions was tested, NaCl was replaced by equimolarity of RbCl, CsCl or LiCl. The currents were recorded using an EPC-10 amplifier with Pulse 8.60 acquisition software and analyzed by Pulsefit 8.60 software (HEKA Electronik, Lambrecht, Germany). Data were filtered at 2 kHz and sampled at 10 kHz. After a whole-cell configuration was established, the cells were held at −70 mV and subject to various protocols as detailed in the text and the figure legends. All experiments were performed at room temperature (~23°C). Tail current analysis was performed to determine reversal potentials (E_{rev}). The cells were first stimulated with +70 mV for 100 ms before stimulation with different potentials (from −120 to +20 or +50 mV). The permeability ratio (P_X/P_K) was determined from E_{rev} according to the Goldman–Hodgkin–Katz equation:

$$E_{rev} = (RT/F)\ln\{([K^+]_o + (P_X/P_K)[X^+]_o)/[K^+]_i\}$$

where R is the universal gas constant, T is the temperature, F is the Faraday constant. $[K^+]_o$ and $[K^+]_i$ represent extracellular and pipette K^+ concentrations, respectively; $[X^+]_o$ represents extracellular concentration of metal ions.

Statistical analysis

Data are presented as mean ± SEM. The unpaired or paired Student's t test was used where appropriate to compare two groups, and a value of $p < 0.05$ was considered to represent a significant difference.

Results

In previous reports, we used HEK293 cells for expression of Kv1.2 WT channels [10, 11]. However, the expression of Kv1.2 V370G was much poorer than the WT. In view of

the endogenous Kv currents in HEK293 cells, we chose OECM-1, a cell line totally devoid of endogenous Kv currents, for channel expression. We did not use CHO cells, as in our hands CHO cells were found to be mechanically rather unstable for recording. Untransfected OECM-1 cells did not express any Kv currents (Fig. 2a, d). After transfection with Kv1.2 WT and V370G, Kv currents expressed (Fig. 2b–d). Kv1.2 V370G currents were much smaller than those of the WT.

The V370 residue of Kv1.2 has been known to have significant effect on C-type inactivation: V370E and V370G mutation accelerates and retards, respectively, C-type inactivation [8, 10]. It is unknown if this residue affects ionic discrimination. We therefore examined if the V370G mutation would affect Kv1.2 channel ion permeability. A tail current analysis of Kv1.2 WT channels expectedly revealed reversal potentials from −62 to −78 mV, with an average of −72 mV (Fig. 3a, c, d). When the mutant V370G channel was examined, large inward tail currents were elicited upon hyperpolarizations, and currents reversed near −9 mV (Fig. 3b–d). Examination of another mutant, V370E, revealed a reversal potential of -57.6 ± 6.1 mV ($n = 3$); since the effect of this mutation was small, it was not further examined.

The very large depolarizing shift of reversal potential in V370G prompted one to ponder if this mutation resulted in non-selective cation permeability. To test this possibility, tail currents were first triggered in the mutant channel in normal bath solution (Fig. 3e). Large inward tail currents could be observed upon hyperpolarization. Subsequently, extracellular Na^+ (140 mM) was entirely replaced with 280 mM sucrose by bath solution exchange, and tail currents were recorded (Fig. 3f). Inward currents were much reduced. A plot of tail currents against voltages revealed a large hyperpolarizing shift of reversal potential upon Na^+ removal (Fig. 3g; quantitative summary in Fig. 3h). After Na^+ removal, reversal potential was converted back to around −80 mV, much closer to the equilibrium potential of K^+. The large shift in reversal potential with Na^+ presence/absence strongly suggests that the V370G mutation endows the Kv1.2 channel with non-selective cation permeability.

Whether the V370G mutant had enhanced permeability to other monovalent cations was further tested. Figure 4a shows the tail current traces of the mutant channel obtained in bath solutions containing 140 mM Rb^+, 140 mM Cs^+ or 140 mM Li^+. Instantaneous I–V curves and quantitative summary of reversal potentials are shown in Fig. 4b, c. A comparison of permeability ratios (P_X/P_K) of WT and V370G is shown in Table 1. The data indicate that the V370G mutation enhanced the permeability to Na^+, Rb^+ and Cs^+. However, V370G mutant channels did not have a significantly augmented permeability to Li^+ when compared with the WT.

Discussion

Our study reports a novel observation that a residue at the pore helix of Kv channel (V370 of Kv1.2) could alter ionic

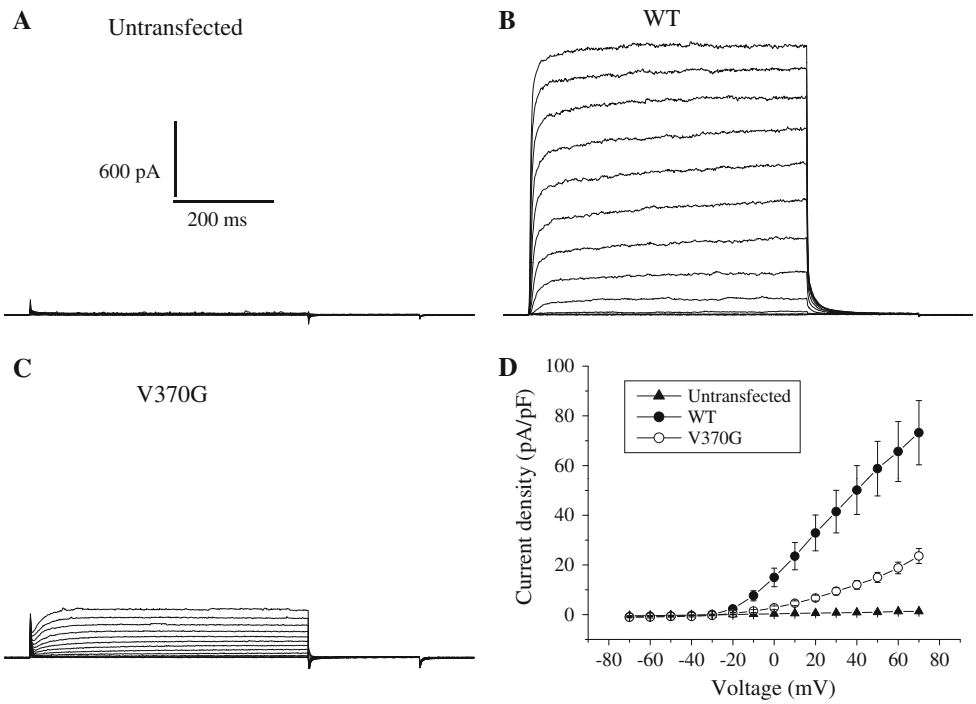

Fig. 2 Expression of WT and V370G Kv1.2 channels in OECM-1 cells Currents were triggered by serial depolarizing voltages in 10 mV increments from a holding potential of −70 mV in **a** untransfected OECM-1 cells, **b** Kv1.2 WT-expressing OECM-1 cells, and **c** Kv1.2 V370G-expressing OECM-1 cells. **d** Current densities are plotted against the applied voltages. Results are mean ± SEM from 9 cells of each group

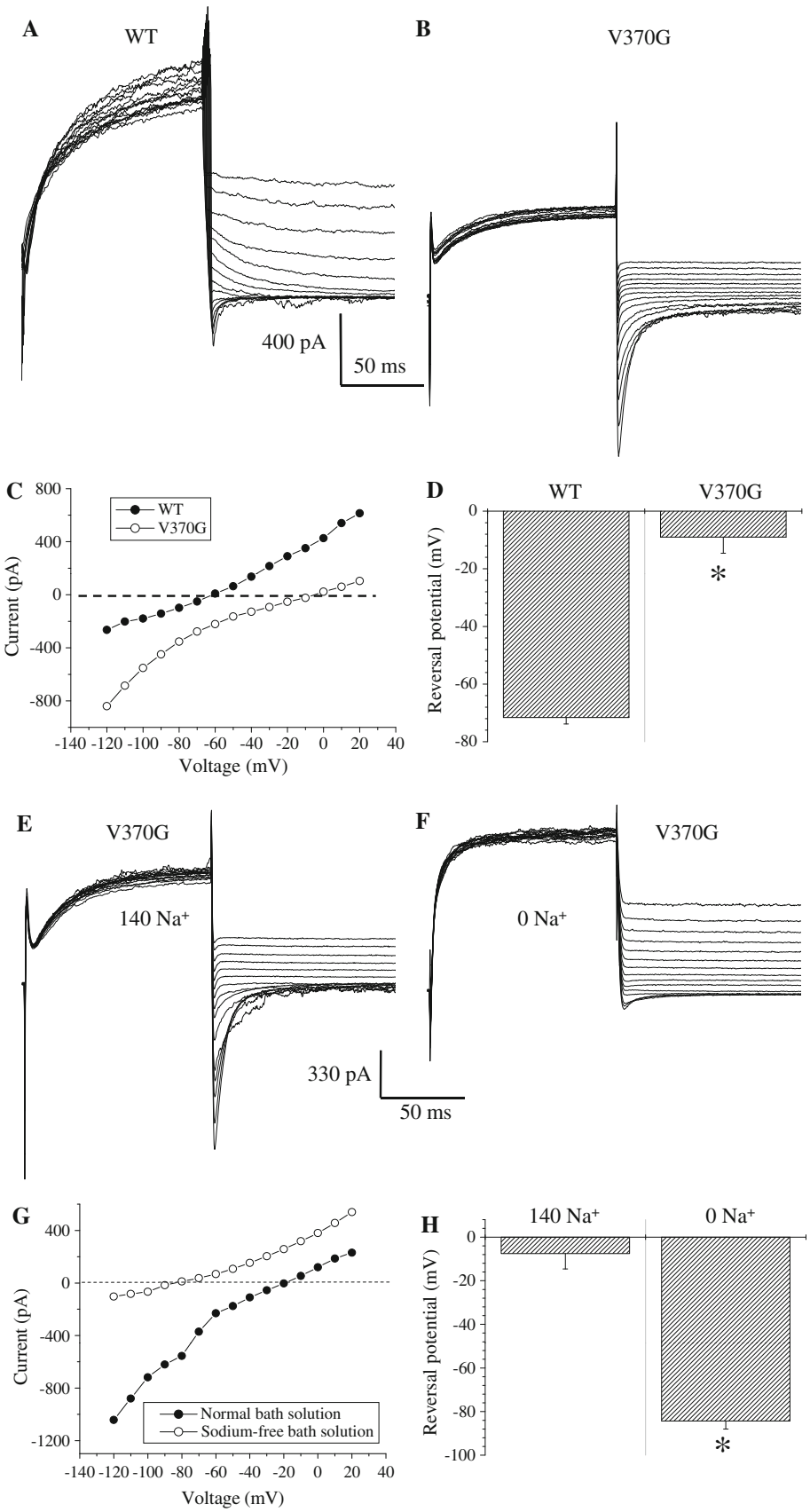

Fig. 3 V370G mutation resulted in non-selective cation conduction in Kv1.2 channels. Cells expressing WT (**a**) or V370G (**b**) Kv1.2 channels were given a pre-pulse of +70 mV to maximally open the channels, followed by voltage steps from −120 to +20 mV at 10 mV increments to yield tail currents. **c** Instantaneous I–V relationships of the tail currents of WT and V370G. **d** Reversal potentials of the tail currents of WT and V370G. Results are mean ± SEM from 7 to 8 cells of each group. *Significantly different from WT ($p < 0.05$). A cell expressing V370G Kv1.2 channels was examined for tail currents in normal 140 mM Na^+-containing bath solution (**e**). The same cell was exposed to a bath solution in which Na^+ ions were completely replaced by 280 mM sucrose (**f**). **g** Instantaneous I–V relationships of the tail currents of V370G in normal and Na^+-free bath solutions. **h** Reversal potentials of the tail currents of V370G in normal and Na^+-free bath solutions. Results are mean ± SEM from 3 cells of each group. *Significantly different from the 140 Na^+ group ($p < 0.05$)

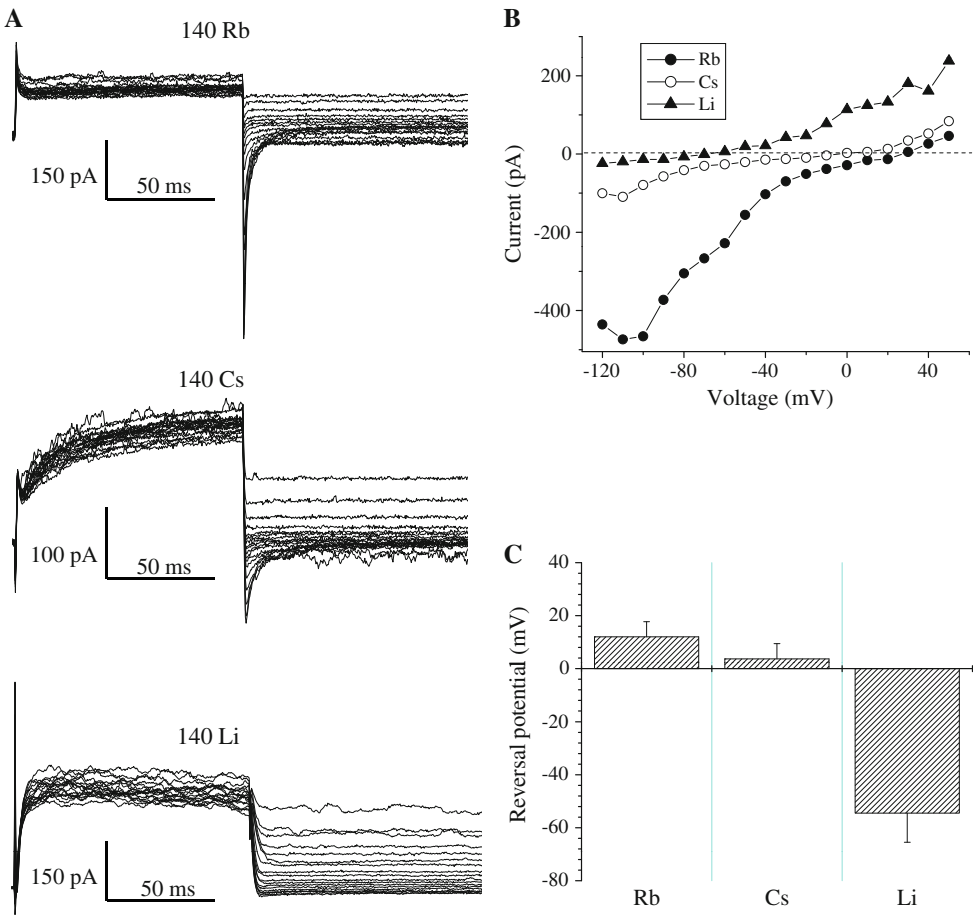

Fig. 4 V370G mutant channels were permeable to Rb^+, Cs^+ but not Li^+. **a** Tail currents of 3 different V370G channel-expressing cells exposed to bath solution containing 140 mM Rb^+, 140 mM Cs^+ or 140 mM Li^+. **b** Instantaneous I–V relationships of the tail currents of V370G in bath solutions containing different cations. **c** Reversal potentials of the tail currents of V370G in bath solutions containing different cations. Results are mean ± SEM from 3 cells of each group

Table 1 Permeability ratios (P_X/P_K) of different cations in Kv1.2 WT and V370G channels

Monovalent cations	WT	V370G
Na^+ (140 mM Na^+, 4 mM K^+)	0.04 ± 0.01	0.76 ± 0.12*
Rb^+ (140 mM Rb^+, 4 mM K^+)	0.78 ± 0.07	1.63 ± 0.33*
Cs^+ (140 mM Cs^+, 4 mM K^+)	0.10 ± 0.02	1.18 ± 0.29*
Li^+ (140 mM Li^+, 4 mM K^+)	0.05 ± 0.01	0.13 ± 0.05

Results are mean ± SEM from 3 to 4 cells of each group

* Significantly different from WT ($p < 0.05$)

permeability, in addition to its role in C-type inactivation [8, 10]. The large shift in reversal potential with Na^+ presence/absence strongly suggests that the V370G mutation endows the Kv1.2 channel with non-selective cation permeability (Fig. 3). The permeability ratio (P_{Na}/P_K) was determined from reversal potentials to be 0.76. Using bath solutions having various cations to substitute for Na^+, we found that the permeability of Kv1.2 V370G to Rb^+ and Cs^+, but not Li^+, was enhanced (Fig. 4; Table 1). It is noted that the V370E mutation, by contrast, only caused a small change in the reversal potential (shifted to −57.6 mV).

Early work in the *Shaker* channel has established that mutations in the 8-amino acid "signature sequence" TMTTVGYG (positions 439–446 of Shaker, equivalent to positions 371–378 in Kv1.2) have various degree of impact on selectivity [12]. Mutations in the first four residues, except for the T439G mutant, leave selectivity unaffected. Mutations in the next four positions result in loss of K^+ selectivity so that the mutants are permeable to Rb^+, Na^+, Li^+, Cs^+ and NH_4^+. We here show, for the first time, that V370 (or its equivalent position) has a very prominent effect on controlling ionic permeability of Kv channels. *Shaker* T439G (equivalent to position 371 of Kv1.2) shows a substantial augmentation in permeability to Cs^+ and NH_4^+, but only a moderate increase in permeability to Na^+, Rb^+ and Li^+ [12]. By contrast, the V370G mutation rendered Kv1.2 channels much more permeable to Na^+, Rb^+ and Cs^+ but still poorly permeable to Li^+.

Kv channels have been known to conduct Na^+ temporarily during C-type inactivation as the selectivity filter constricts [7]. Our data show that the Kv1.2 V370G mutant, having reduced C-type inactivation [10], could allow the passage of Na^+. The mechanism by which Na^+ passes is yet to be determined. It is important to note that mutation in the Asp379 equivalent in Kv2.1 (Asp378)

results in a modest loss of selectivity [13]. Hence, interaction between the selectivity filter and adjacent pore helix appears important in controlling ionic selectivity.

It has been shown that Kv3.1 Y407 is responsible for $NMDG^+$ permeability in the absence of K^+ [9]. Equivalent mutation in Kv1.5 (R487Y) (equivalent to V381 in Kv1.2) endows the channel with $NMDG^+$ conductivity [9]. A recent work by Backx's group indicates that TVGYG does not suffice to confer K^+ selectivity in the Na^+–K^+ co-permeable HCN4 channels [14]. Introduction into HCN4 channels of mutations that also enhance Kv channel selectivity filter stability still failed to endow K^+ selectivity, implicating that differences between HCN and Kv channels may be ascribed to domains remote to the selectivity filter [14]. In conclusion, V370 in the pore helix adjacent to the selectivity filter of the Kv1.2 channel is important not only for inactivation gating [8, 10] but also for ionic selectivity.

Acknowledgments Y.M.L. would like to thank China Medical University, Taiwan, and the Taiwan National Science Council for providing research funds (CMU97-340; CMU98-S-29; NSC 97-2320-B-039-029-MY3). C.C.C. is a recipient of a Hsing Tian Kong Scholarship. We thank Dr M.J. Hour and Mr. T.L. Chen for their help in molecular graphics.

References

1. Hille B (2001) Ion channels of excitable membranes, 3rd edn. Sinauer, Sunderland
2. Choe S, Kreusch A, Pfaffinger PJ (1999) Towards the three-dimensional structure of voltage-gated potassium channels. Trends Biochem Sci 24:345–349
3. Choe S (2002) Potassium channel structures. Nat Rev Neurosci 3:115–121
4. Yellen G (2002) The voltage-gated potassium channels and their relatives. Nature 419:35–42
5. Hoshi T, Zagotta WN, Aldrich RW (1990) Biophysical and molecular mechanisms of Shaker potassium channel inactivation. Science 250:533–538
6. Kurata HT, Fedida D (2006) A structural interpretation of voltage-gated potassium channel inactivation. Prog Biophys Mol Biol 92:185–208
7. Kiss L, LoTurco J, Korn SJ (1999) Contribution of the selectivity filter to inactivation in potassium channels. Biophys J 76:253–263
8. Cordero-Morales JF, Jogini V, Lewis A, Vasquez V, Cortes DM, Roux B, Perozo E (2007) Molecular driving forces determining potassium channel slow inactivation. Nat Struct Mol Biol 14:1062–1069
9. Wang Z, Wong NC, Cheng Y, Kehl SJ, Fedida D (2009) Control of voltage-gated K^+ channel permeability to $NMDG^+$ by a residue at the outer pore. J Gen Physiol 133:361–374
10. Leung YM, Wong KL, Lin CH, Chao CC, Chou CH, Chang LY, Chen SW, Cheng TH, Kuo YH (2010) Dependence of 6beta-acetoxy-7alpha-hydroxyroyleanone block of Kv1.2 channels on C-type inactivation. Cell Mol Life Sci 67:147–156
11. Chou CH, Gong CL, Chao CC, Lin CH, Kwan CY, Hsieh CL, Leung YM (2009) Rhynchophylline from *Uncaria rhynchophylla* functionally turns delayed rectifiers into A-type K(+) channels. J Nat Prod 72:830–834
12. Heginbotham L, Lu Z, Abramson T, MacKinnon R (1994) Mutations in the K^+ channel signature sequence. Biophys J 66:1061–1067
13. Kirsch GE, Pascual JM, Shieh CC (1995) Functional role of a conserved aspartate in the external mouth of voltage-gated potassium channels. Biophys J 68:1804–1813
14. D'Avanzo N, Pekhletski R, Backx PH (2009) P-loop residues critical for selectivity in K channels fail to confer selectivity to rabbit HCN4 channels. PLoS One 4:e7712